PNAS
www.pnas.org

Supplementary Information for

Emerging forest-peatland bi-stability and resilience of European peatland carbon stores.

Ype van der Velde, Arnaud J.A.M. Temme, Jelmer J. Nijp, Maarten Braakhekke, George A.K. van Voorn, Stefan C. Dekker, A. Johannes Dolman, Jakob Wallinga, Kevin J. Devito, Nick. Kettridge, Carl A. Mendoza, Lammert Kooistra, Merel B. Soons, Adriaan J. Teuling.

Email: Ype.vander.Velde@VU.nl

This PDF file includes:

Supplementary texts S1-S5

Supplement 1: Model setup

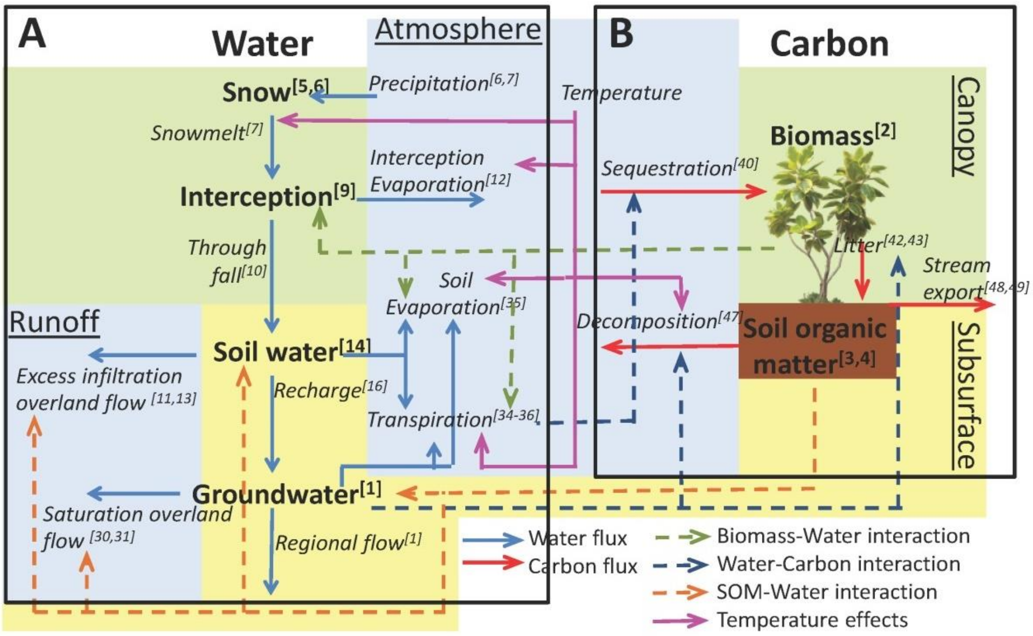

Figure S1.1 Conceptual diagram of model relationships. Panel A shows the simulated stores (bold text) and flows of water (blue arrows), Panel B shows the simulated stores (bold texts) and flows of carbon (red arrows). The dotted lines present the simulated interactions between the water and carbon cycles. The purple arrows indicate how temperature affect the model. The numbers refer to the corresponding equations.

The model (Fig S1.1) is centered around 4 main differential equations. These describe the mass balances of water [1], carbon in the vegetation [2] and carbon in the soil [3] and the surface elevation [4]. The same equations and parameters values are used for both forest and peatland, which are treated as a continuum in living biomass, with forest as a high biomass and peatland with a low living biomass. Therefore by growing biomass a peatland can develop into a forest and vice-versa.

Ground water: $$\frac{\partial H}{\partial t} = \frac{R-(E_{gr}+T_{gr})-Q-J}{Sy} \quad [1]$$

Biomass: $$\frac{\partial B}{\partial t} = Npp - M - Wd \quad [2]$$

Soil Organic matter: $$\frac{\partial O}{\partial t} = M + Wd - D - Se \quad [3]$$

Soil Surface $$S = Ms + Sod \text{ or equivalent } \frac{\partial S}{\partial t} = \frac{1}{\rho}\frac{\partial O}{\partial t} \quad [4]$$

Table S1.1: Main variables

H	Groundwater level [m]	***R***	Groundwater Recharge [m/d]	***M***	Maintenance of biomass [KgC/m^2/Y]
B	Biomass [Kg C/m^2]	E_{gr}	Evaporation from groundwater [m/d]	***Ws***	Death of biomass through both too wet and too dry conditions [KgC/m^2/Y]
O	Soil organic matter content [Kg C/m^2]	T_{gr}	Transpiration from groundwater [m/d]	***D***	Decay of soil organic matter [KgC/m^2/Y]
S	Soil Surface [m]	***Q***	Discharge [m/d]	***Se***	Stream export of organic matter [Kg/m^2/Y]
T	Time [d or Y]	***J***	Regional flux[m/d]	***Ms***	Mineral surface [m]
Sy	Specific yield [-]	***Npp***	Biomass growth [Kg/m^2/Y]	***Sod***	Depth soil organic layer [m]

Interaction model equations

Here we describe all the interactions (arrows in Fig. S1) linking the state variables.

Water

The point-scale hydrology is schematized by 4 serial reservoirs (figure S1.1, panel A): Snow, interception, soil water and groundwater. If the temperature is below zero, precipitation accumulates in the snow reservoir, from which it leaves during periods when temperature is above zero following the degree-day approach (Collins, 1934).

$$\frac{dSn}{dt} = -\min(Sn, Tmp \cdot f_{SN}) \qquad Tmp > 0 \qquad [5]$$

$$\frac{dSn}{dt} = P \qquad Tmp <= 0 \qquad [6]$$

$$P_S = P + \min(Sn, Tmp \cdot f_{SN} dt) \qquad Tmp > 0 \qquad [7]$$

$$P_S = 0 \qquad Tmp <= 0 \qquad [8]$$

Interception storage is included via a threshold storage approach (Moors, 2012; Vrugt et al., 2003)

$$\frac{dI}{dt} = P_S - E_I - Tf \qquad [9]$$

$$Tf = \max(P_S - (I_{max} - I), 0) \qquad [10]$$

$$Of = \max(Tf - W_{\max}, 0) \qquad [11]$$

$$E_I = \min(Et_P, I) \qquad [12]$$

$$W_{\max} = f_{W1} + f_{W2} \cdot (B + O) \qquad [13]$$

$$I_{\max} = f_I \cdot B \qquad [14]$$

Unsaturated soil water storage is again implemented via a threshold storage approach. Soil organic matter and average groundwater depth increase the capacity of this store. Conceptually the volume of the store represents the volume of water that vegetation can easily use from the unsaturated zone. Water leaking from this store becomes groundwater recharge.

When the vegetation cannot reach groundwater it will use the water in this unsaturated store to transpire and grow:

$$\frac{\mathrm{d}\,Sw}{\mathrm{d}\,t} = Tf - Of - Et_S - R \qquad [15]$$

$$R = \max(Tf - Of - Et_S - (Sw_{\max} - Sw), 0) \qquad [16]$$

$$Sw_{\max} = \min(Sod, S - \overline{H}) * f_{SW1} + \max(S - \overline{H_l}, 0) * f_{SW2} \qquad [17]$$

$$Sod = \left[\sqrt{2 \cdot d\rho_C \cdot O + \rho_0^{\ 2}} - \rho_0\right] / d\rho_C \qquad [18]$$

$$Et_S = \min(Et_P - Et_I, Sw) \qquad [19]$$

$$Et_P = Et_R \cdot \left(f_{Et1} + \min(f_{Et2} \cdot B, f_{Et3} - f_{Et1})\right) \qquad [20]$$

Groundwater Evaporation and transpiration are implemented building on the Feddes approach (Bartholomeus et al., 2008; Feddes et al., 2001). The rootzone thickness is modelled as a function of biomass following (Roebroek et al., 2020) ::

$$ET_{Gr} = j \cdot (Et_P - Et_S - Et_I) \qquad [21]$$

$$Gd_{1,2,3} = f_{Gd1,2,3} \cdot B \qquad [22]$$

$$j = j_0 \qquad \text{H > S} \qquad [23]$$

$$j = j_0 + \frac{S - H}{Gd_1}(1 - j_0) \qquad \text{S-Gd}_1(B) < \text{H} < \text{S} \qquad [24]$$

$$j = 1 \qquad \text{S-Gd}_2(B) < \text{H} < \text{S-Gd}_1(B) \qquad [25]$$

$$j = 1 - \frac{S - H - Gd_2}{Gd_3 - Gd_2} \qquad \text{S-Gd}_3(B) < \text{H} < \text{S-Gd}_2(B) \qquad [26]$$

$$j = 0 \qquad \text{H} < \text{S-Gd}_3(B) \qquad [27]$$

$$T_{Gr} = \left(f_{T0} + (f_{T\max} - f_{T0})\frac{S - H}{S - f_{TH}}\right) ET_{Gr} \qquad [28]$$

$$E_{Gr} = ET_{Gr} - T_{Gr} \qquad [29]$$

Discharge is calculated as a linear reservoir when groundwater reaches above surface following (Van Der Velde et al., 2009)

$$Q = Rw \cdot (H - S) + Of \ \text{ for H >S,} \qquad Q = Of \ \text{ for H< S} \qquad [30]$$

$$Rw = \max(f_{Rw1} - f_{Rw2} \cdot Sod, f_{Rw3}) \qquad [31]$$

Specific yield of the soil is a thickness dependent linear combination of mineral and peatland specific yield:

$$Sy = \min(Sy_0 + \frac{SOD}{f_p}(Sy_p - Sy_0), Sy_p) \qquad [32]$$

Biomass
Living biomass is calculated on a yearly basis following a Water use efficiency approach following results of e.g. (Mueller et al., 2005; Tang et al., 2015) :

$$\frac{\partial B}{\partial t} = Npp - M - Wd \qquad [2]$$

Yearly averages and sums:

$$\overline{\overline{H}} = \frac{\sum_{i=1}^{nt} H(i)}{nt} \qquad [33]$$

$$\overline{\overline{T_{Gr}}} = \sum_{i=1}^{nt} T_{gr}(i) \qquad [34]$$

$$\overline{\overline{T}}_S = \left(f_{T0} + (f_{T\max} - f_{T0}) \frac{S - \overline{\overline{H}}}{S - f_H} \right) \sum_{i=1}^{nt} Et_S(i) \qquad [35]$$

$$\overline{\overline{E}} = \sum_{i=1}^{nt} Et_S(i) - \overline{\overline{T_S}} + \sum_{i=1}^{nt} E_{Gr}(i) \qquad [35]$$

$$\overline{\overline{T}} = \overline{\overline{T_{Gr}}} + \overline{\overline{T_S}} \qquad [36]$$

$$\overline{\overline{E_{stress}}} = \overline{\overline{ET_p}} - \overline{\overline{ET_{gr}}} - \overline{\overline{ET_S}} - \overline{\overline{E_I}} \qquad [37]$$

$$T_{tresh} = T_0 \cdot \left(1 - e^{-f_{TS} B}\right) \qquad [38]$$

Biomass Growth

$$Npp = \frac{\overline{\overline{T}} - T_{tresh}}{Wue} \qquad [39]$$

$$Wue = Wue_{NS} + (1 - f_{WUE1}) \cdot f_{WUE2} \cdot \overline{\overline{E_{stress}}} \qquad [40]$$

Maintenance cost biomass:

$$M(B) = f_M \cdot B \qquad [41]$$

Water stress related biomass death:

$$WD = \frac{S - \min(\max(S - \overline{\overline{H}}, 0), Gd_1)}{S - Gd_1} \cdot f_{WD1} \cdot B + Di \qquad [42]$$

Where *Di* represents the fraction of *Npp* that ends up on the soil in the same year due to water stress.

$$Di = Npp - \frac{\overline{\overline{T}} - T_{tresh}}{Wue_{NS} + f_{WUE2} \cdot \overline{\overline{E_{stress}}}} \qquad [43]$$

Soil Organic matter

$$\frac{\partial O}{\partial t} = M + Wd - D - Se \qquad [3]$$

Decomposition is calculated following the acrotelm and catotelm approach outlined by (Clymo, 1984) and for example applied by (Kleinen et al., 2012)

$$O_{dry} = \min(\max(S - \overline{H}, 0), Sod) \cdot \rho_0 + \frac{\rho_c}{2} \min(\max(S - \overline{H}, 0), Sod)^2 \quad [44]$$

$$O_{wet} = O - O_{dry} \quad [45]$$

$$D = \cdot f_{Ow} \cdot 2^{\frac{\overline{Tmp} - 10}{10}} \cdot O_{wet} + f_{Od} \cdot 2^{\frac{\overline{Tmp} - 10}{10}} \cdot O_{dry} \quad [46]$$

Stream export is calculated by assuming a water residence time dependent DOC concentration following (van der Velde et al., 2010):

$$mtt = \frac{\min(Sod, f_{SE1}) \cdot Sy_p}{\overline{\overline{Q}}} \quad [47]$$

$$SE = Q \cdot C_{eq} \int_0^{Inf} \frac{1}{mtt} e^{-\frac{x}{mtt}} (1 - e^{-f_{SE2} x}) dx \quad [48]$$

Table S1.2 All variables

Variables	**Interpretation**
[E]	Yearly sum of total evaporation [m/Y]
[E_I]	Yearly sum of evaporation from interception storage [m/Y]
[E_{stress}]	Yearly sum of water stress due to too wet and/or too dry conditions [m/Y]
[H]	Yearly average groundwater level [m]
[H_l]	Yearly average groundwater level of last year [m]
[Q]	Yearly sum of discharge [m/Y]
[T]	Yearly sum of total transpiration [m/Y]
[Tmp]	Yearly average temperature [C]
[T_S]	Yearly sum of Transpiration from SW [m/Y]
B	Living biomass [KgC/m^2]
Di	Input of organic matter to the soil due to transpiration deficit [KgC/m^2/Y]
E_{Gr}	Evaporation from groundwater [m/d]
E_I	Evaporation from interception [m/d]
Et_{Gr}	Evapotranspiration from groundwater [m/d]
Et_p	Potential evapotranspiration of biomass (not water limited) [m/d]
Et_R	Reference evapotranspiration of a not water limited grass field [m/d]
Et_S	Evapotranspiration from SW [m/d]
H	Groundwater level [m]
I	Interception storage [m]
I_{max}	Maximum interception storage [m]
j	Reduction factor for Evapotranspiration from groundwater depending on groundwater dept hand biomass [-].
J	Regional flux of water (seepage is negative, infiltration is positive) [m/d]
mtt	Mean traveltime of water in the upper organic layer [Y]
Npp	Net primary production [KgC/m^2/Y]
O	Soil organic matter [Kg/m^2]
O_{dry}	Soil organic matter above yearly average groundwater table [KgC/m^2]
Of	Overlandflow [m/d]

O_{wet}	Soil organic matter below yearly average groundwater table [KgC/m^2]
P	Precipitation [m/d]
P_S	Non-frozen Precipitation + snowmelt [m/d]
Q	Discharge [m/d]
R	Recharge from SW to groundwater [m/d]
Rw	Conductivity of soil surface against exfiltration of groundwater when groundwater level is above soil surface, S [d]
S	Surface elevation [m]
Se	Stream export of organic matter [KgC/m^2/Y]
Sn	Snow storage [m]
Sod	Depth of soil organic layer [m]
Sw	Unsaturated soil water storage above field capacity of mineral soil [m/d]
Sw_{max}	Maximum SW storage [m]
T	time [d for hydrology / Y for Biomass and soil organic matter]
Tf	Throughfall: flow from interception to soil [m/d]
T_{Gr}	Transpiration from groundwater [m/d]
Tmp	Temperature [C]
T_{thres}	Biomass dependent threshold in transpiration needed at begin of season before growth starts. The more biomass, the higher this threshold [m/Y].
Wd	Input of organic matter from biomass to soil due to too wet and/or too dry conditions [kgC/m^2/d]
W_{max}	Maximum infiltration [m/d]
Wue	Water use efficiency: effective transpiration needed for 1 Kg of NPP [m/kg]
nt	Number of time steps in year

Table S1.3 All parameters

Constants	**Estimated value**	**Interpretation**	**Reference**
C_{eq}	0.045 Kg C/m^3	Equilibrium carbon concentration after infinit residence time of water in the unsaturated zone	Maximum concentration from Supplement 2
$d\rho_c$	12.5 Kg C/m^3/m	Increase in dry Carbon density of organic matter with depth.	(Steve Frolking et al., 2001)
f_{ET1}	0.7 [-]	Potential ET without Biomass	Based on (Teuling, 2017)
f_{ET2}	0.2 1/kg	Increase in ETp with Biomass	Based on (Teuling, 2017)
f_{ET3}	1.4 [-]	Max ETp with Biomass	Based on (Teuling, 2017)
f_{Gd1}	0.05 m/KgC	Groundwater above this level (*B) reduces ET due to oxygen stress.	Based on (Bartholomeus et al., 2008)
f_{Gd2}	0.12 m/KgC	Groundwater below this level (*B) reduces ET due to water stress.	Based on (Bartholomeus et al., 2008)
f_{Gd3}	0.2 m/KgC	Groundwater below this level (*B) reduces ET to 0.	Based on (Bartholomeus et al., 2008)

f_I	3500 Kg/m^2/m	Biomass needed for 1m of interception	(Moors, 2012)
f_M	0.07 [1/Y]	Fraction of biomass that dies per year	This study, based on forest biomass data.
f_{Od}	0.08 [1/Y]	Decay rate of soil organic matter above water table	(Kleinen et al., 2012)
f_{Ow}	6.5*10^{-5} [1/Y]	Decay rate of soil organic matter below water table	(Clymo, 1984)
f_p	1 m	Thickness of organic soil needed to fully change from p_0 to p_p [-]	This study. Based on typical groundwater level fluctuations in peatlands. When> 1m, groundwater level usually stays inside the peatlayer.
f_{RW1}	50 d	Exfiltration resistance of mineral soil	(Van Der Velde et al., 2009)
f_{RW2}	0 d	Exfiltration resistance increase per meter of soil organic layer	With this value this parameters does not affect simulation
f_{RW3}	50d (not used in simulations)	Maximum exfiltration resistance	With this value this parameters does not affect simulation
f_{SE1}	2 [1/Y]	Fractional uptake rate of carbon by rainwater	This study
f_{SE2}	0.6 m	Maximum flow depth with thick organic layers	Loosely based on (Beckwith et al., 2003)
f_{sn}	0.002 m/C	Meter snowmelt per degree above zero	Collins et al., 1934
f_{SW1}	0.08 [m/m]	Available extra soilwater per meter of soil organic matter	(Kätterer et al., 2006)
f_{SW2}	0.002 [m/m]	Available extra soilwater per meter of soil above water table. This parameter controls Biomass growth under dry conditions	This study, based on forest biomass of dry forests that cannot use groundwater and thus grow on unsaturated storage
f_{T0}	0.135 [-]	Fraction of transpiration from ET when groundwater level is at or above surface	This study, based on *Npp* and *Et* values of peatlands
f_{TH}	0.3 m	Depth above which increase in direct evaporation from groundwater occurs.	This study, based on *Npp* and *Et* values of peatlands
f_{Tmax}	0.95 [-]	Fraction of transpiration from total ET when groundwater level is below f_{TH}	Based on (Bartholomeus et al., 2008)
f_{TS}	0.5 1/KgC	Describes relation between Biomass and transpiration threshold	This study, based on forest biomass data (fig 2.1a)

f_{W1}	0.01 m/d	Infiltration capacity of mineral soil	Representative value, idea from (Siteur et al., 2014)
f_{W2}	0.003 m/d/KgC	Increase in infiltration capacity per Kg of stored organic carbon.	(Siteur et al., 2014)
f_{WD1}	0.25 [1/Y]	Maximum fraction biomass death due to water at surface per year	This study, estimated. Controls speed of transition between forests and peatlands
f_{WUE1}	0.8 [-]	Fraction of [E_{stress}] that increases litter input	This study, based on soil organic matter data for the warmer climates with water stress
f_{WUE2}	0.7 [-]	Fraction of [E_{stress}] that decreases WUE	This study, based on the forest biomass data under warmer climates
j_0	0.75 [-]	Fraction ET when water table at or above surface	Based on f_{ET1} + results in (Lafleur et al., 2005)
Ms	10 m	Surface of the mineral soil	Arbitrary
Sy_0	0.17 [-]	Specific yield of mineral soil	Representative value
Sy_p	0.6 [-]	Specific yield of top layer peat	(Bourgault et al., 2017; Clymo, 1984)
T_0	0.220 m	Threshold in transpiration needed at begin of season before growth starts for a full grown forest. [m/Y].	(Mueller et al., 2005)
Wue_{NS}	0.160 m/KgC	Water use efficiency if there is no water stress (dry or wet)	(Mueller et al., 2005)
ρ_0	25 Kg C/m^3	Dry Carbon density of top layer organic matter.	(S Frolking et al., 2010)

Supplement 2. Model example.

An example model result for De Bilt, Netherlands (5.2Lon, 52.1Lat), is shown in figure S2.1. Panel A shows times series of living Biomass. Here we see that full switches from peatland to forest and vice versa may take several centuries. The bi-stability diagram in figure S2.1B plots the average biomass after 800-1000y of simulation (not shown in fig. A)

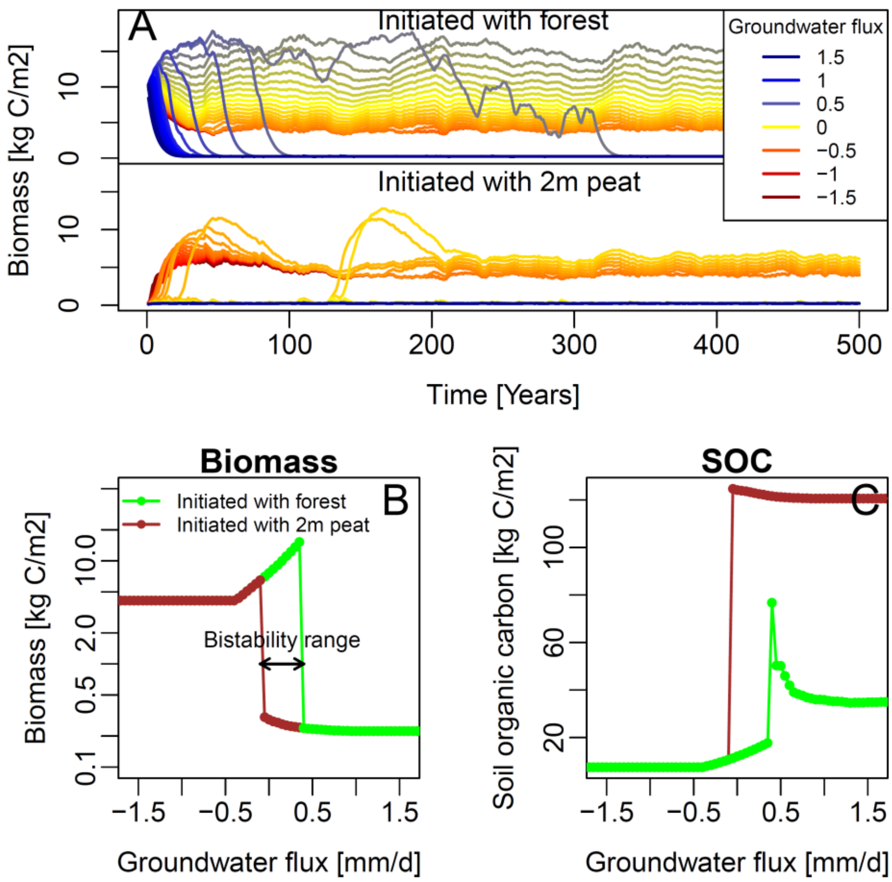

Figure S2.1) Example model run and its relations to the biomass bi-stability diagrams. A) time series of modelled biomass for different "Regional fluxes". B) Bi-stability diagram for biomass demonstrating the definition of "bi-stability range". Each point represents the average biomass for 800-1000Y simulation for 1 of the simulations shown in A. the green dots are initiated with a typical forest, while the brown points are initiated with a typical peatland C) Average soil organic matter after 800-1000Y of simulations for the simulations shown under A.

In figure S2.1A the biomass of the individual model runs for a single location are shown. The model is run with 2 starting conditions:1) a forest with high biomass, a high groundwater table and a thin organic soil and 2) peatland with low biomass, high groundwater table and a thick organic soil. For each of the starting conditions 40 model runs are performed with groundwater flow varying in equal steps from 2mm/d infiltration (negative) to 2 mm/d exfiltration (positive) Most model runs find their stable state within the first 100years of simulation. A few model runs switch form forest to peatland or from peatland to forest much later signaling that the generated weather (the years 1955-2015 were placed in random order to create a 1000 years of weather, all models were run with the same weather input) was such that switches were induced for example by the coincidence of having multiple wet or dry years in a row. The average biomass and soil organic carbon during the time period of 800-1000y of simulation was plot in the bi-stability plots of figs S2.1B. The biomass of forest is constant for a groundwater flux more negative than -0.5mm/d (infiltration). For these groundwater fluxes, the groundwater table is below the rootzone of the trees and trees grow only with the water present in the unsaturated zone, thus unaffected by the groundwater flux. From a groundwater flux of -0.5 to +0.5 mm/d, the biomass of the forests increases non-linearly (note the logscale of the y-axis of Fig S2.1B). Here, the trees can access the groundwater and grow to a higher biomass. Up to an exfiltration flux of 0.5mm/d the trees grow taller. The higher biomass of the trees and the more wet conditions also create the peak in soil organic carbon as function of groundwater flux (Fig 2.1C). Increasing the exfiltration even further shows a sudden drop in biomass. However, fig S2.1A shows that in time this is not a sudden drop in biomass and soil organic carbon but a transition that potentially takes hundreds of years.

Supplement 3 Model verification and validation,

S3.1 Water and carbon stores and fluxes.

We tuned the parameters that describe the relationships between biomass, water table evapotranspiration and growth within their uncertainty ranges to match observed data for Europe (Fig. S3.1). This setup was subsequently validated for Canadian datasets (Fig. S3.2) as the number of suitable datasets in Europe is limited. Moreover, demonstrating that the model works well under contrasting climatic conditions builds confidence in our model results.

S3.1.1 Verification for Europe

The full range of likely wetness condition was evaluated for each observation site. As it is difficult to assess the wetness condition for each observation site from literature, we aim our model to envelope the forest observations. To this end we plotted the highest (no water stress) and lowest (max water stress) simulated biomass, NPP and forest soil carbon and compared these with the observed values. Ideally our model envelopes the observations, which it does wel for Biomass, NPP and soil carbon (Fig S3.1). For waterfluxes, we compared primarily with observed river runoff in Sweden. These river discharges of more than400 rivers were first analyzed to yield water use (actual evapotranspiration, AET) of the forest and wetland parts of the catchments. These water fluxes, and the water fluxes obtained from several fluxnet-sites, were compared with the simulated water fluxes for forest and peatlands (Fig S3.1d). Lastly the simulated carbon fluxes of the peatlands were compared with data found through a literature review of peatland research within Europe.

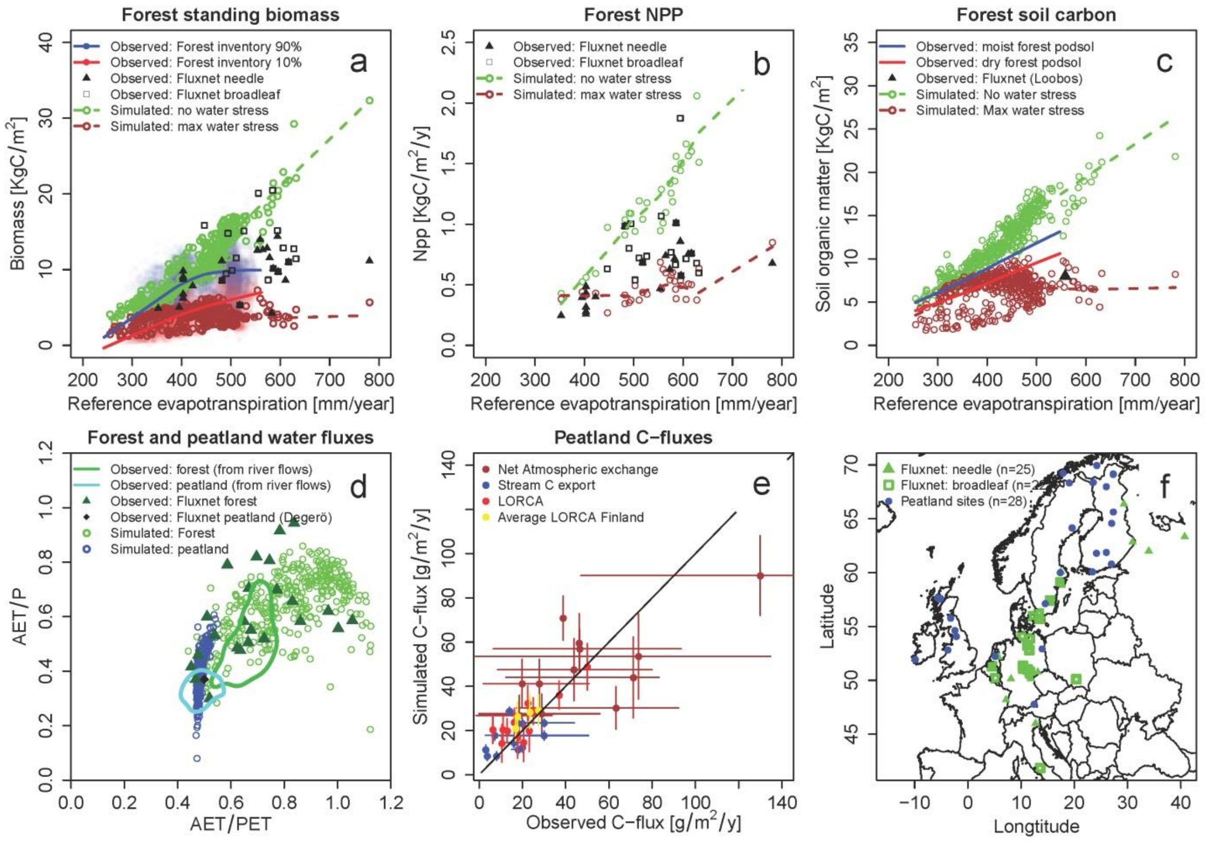

Figure S3.1 Figs S3.1a,b,d,e are a copy of figure panels in Fig. 2 of the main text. For completeness they are repeated here. Model verification results for forest and wetland ecosystem properties.

*A) Modelled forest biomass were compared with 2 datasets of measured forest biomass.1) Forest biomass inventories of Sweden (ftp://salix.slu.se/download/skogskarta, downloaded in 2015) on a 25*25m grid are upscaled to 10 by 10Km grid. For each 10 by 10 Km gridcell the 0.1 percentile (10%) and 0.9 percentile (90%) of forests biomass for forests that are more than 60 years* *old are calculated. The 0.1 percentile is assumed to compare to simulated forests that cannot use groundwater and hence are dry forests (“no-groundwater” scenario) , while the 0.9 percentile is assumed to correspond to simulated forests that are optimally supplied with water throughout the growing season (“optimal-water-supply”-scenario). Both simulated and measured forests biomasses are shown and compare well. 2) Biomass of European forest fluxnet sites with trees older than 60 years are compared with simulated biomass (Luyssaert et al. 2007). Both model scenarios are expected to envelope the fluxnet sites as these sites are likely to have some degree of groundwater use and or water limitation during the growing season.*

B) *Net primary production (Npp) of the model were compared with forest Npp values from the fluxnet sites with trees older than 60y (Luyssaert et al. 2007). Just as under A, the “no-groundwater” and the “optimal-water-supply” scenarios of our model are expected to envelope the fluxnet sites.*

C) *Simulated Forest soil organic carbon stocks were compared with published latitude-“forest-soil-carbon-stock” relationships for both moist and dry podsols in Sweden (Olsen et al., 2009). The moist podsol relationship is expected to correspond with the ”optimal-water-supply” scenario of our model, while the “dry-podsol-forest-carbon-stocks” are expected to correspond to our “No-groundwater” scenario. Note that the published average relationships have a large uncertainty. This uncertainty could not be quantified from the publication.*

D) *Simulated forest and peatland water fluxes were compared to 2 types of measured water fluxes. 1) Forest and wetland water use derived from river discharges throughout Sweden (Van der Velde et al, 2013) 2) Forest water use derived from fluxnet sites (Williams et al,, 2012). For the forest compared the simulations with “regional flux” = 0.*

E) *Peatland carbon fluxes were obtained through a literature review (see table S2.1).Net Atmospheric exchange (NAE), DOC export through rivers and LORCA (long term rate of carbon accumulation) were collected for a range of sites. In Finland a large number of Lorca values were determined by Turunen et al, 2002 (>1000). Here average values are used for the regions specified in the publication. The whiskers on the observations indicate the range in yearly values when multiple years are measured. The whiskers on the simultations indicate the standard diaviation between years in the simulation.*

F) *Overview map of the used European sites*

Table S3.1 European peatland carbon flux data.

Site	Lat	Lon	NAE	NAE_{min} gC/m^2/y	NAE_{max} gC/m^2/y	NAE_{SD} gC/m^2/y	DOC gC/m^2/y	DOC_{min} gC/m^2/y	DOC_{max} gC/m^2/y	DOC_{sd} gC/m^2/y	LORCA gC/m^2/y	avLorca gC/m^2/y	Reference
Glencar	51.96	-9.9	47.8	12.5	84	30	14	13	16.5	1.6			Helfter et al, 2015
Degero	64.18	19.55	58	18	105		18	15	20	1.3			Helfter et al, 2015
Stordahlen	68.35	19.04	66	20	95		3	2.76	3.56	0.3			Olefeldt et al, 2012
KipoJarvi	69.19	27.3	30.8				3.7				6.3		Juutinen et al, 2013
Auchencorth	55.79	-3.25	74	-20	135		30	20	37	20.6			Helfter et al, 2015
Andoya	69.25	17.87	20.6	0.5	35.7	18.6	7.2	2.8	18.7				De Wit et al, 2016
Moor house	54.65	-2.45	79	20	91		30	17	44				Billet et al, 2010
Conwy	52.83	-3.76					20						Billet et al, 2010
Akhult mire	57.14	14.53	43				20						Malmer et al, 2011
Horstermeer	52.24	5.08	300	232	446		16			4.3			
Kamaanen	69.14	27.3	22	4	53		8				11		Aurela et al, 2004
Kendlmuhlfilzen	47.8	12.44	150	67	183								Drösler et al, 2005
Lompolojänkkä	69.97	24.2	32	3	59								Helfter et al, 2015
Siikaneva	61.82	24.14	51.2										Aurela et al, 2004
The Glen Carron	57.62	-5.15									10.5		Yu et al, 2010
The Glen Torridon	57.57	-5.37									20.5		Yu et al, 2010
The Eilean Subbainn	57.68	-5.68									17.7		Yu et al, 2010
Hanhijänk	68.4	23.55									13		Yu et al, 2010
Haukkasu	60.82	26.95									22.5		Yu et al, 2010
Ruosuo	65.65	27.32									16.2		Yu et al, 2010
Malham Tarn	54.09	-2.17									23.11		Turner et al, 2013
Lappmyran	64.16	19.59									25		Van der Linden et al, 2014
Åkerlänna	60.02	17.35									37		Van der Linden et al, 2014
Barschpfuhl	52.94	13.95									50		Van der Linden et al, 2014

Finland A	60.09	23.4										23.4	Turunen et al, 2002
Finland C	61.9	26										27.4	Turunen et al, 2002
Finland D	64.6	27										17.8	Turunen et al, 2002
Finland E-H	68	26										16.9	Turunen et al, 2002
Sweden Skåne	56.25	13.55	21			5.4							Wang et al, 2018
Germany Bavaria	47.8	11.32	62										Wang et al, 2018
Ireland Kerry	51.92	9.92	55.7			18.9							Wang et al, 2018

S3.1.2 Validation against Canadian datasets

Similar to the model verification in Europe, we validated the European model with Canadian datasets. Simulated standing forest biomass is compared to both a gridded forest biomass map and site measurements (fig S3.2). Our simulations envelope most site biomass observations (FECD) but suggests that most forests in the gridded forest biomass map are water stresses. However, other explanation are more likely, such as an averaging effect over 250 by 250m grid cells, cold soil and winter temperatures at locations with low reference evapotranspiration that affects biomass. The simulations accurately envelope observed forest NPP and forest soil carbon. The European model accurately describes the water usage of peatlands AET/PET ~0.6 that corresponds well with flux tower and water balance measurements. This peatland water use is controlled by the standing biomass and weather dynamics. The forest water use corresponds less well and the simulations seem to slightly overestimate water use of forest. A likely explanation is that winters in Canada are colder than in Europe. Cold soils may limit water use of trees, a process that is not incorporate in the model. The simulated NEE of peatlands is higher than carbon accumulation estimated by dating techniques (LORCA), but matches fairly well to fluxtower measurements (observed NEE). This discrepancy could be explained by long-term carbon-loss processes that were not accounted for in the model such as fires.

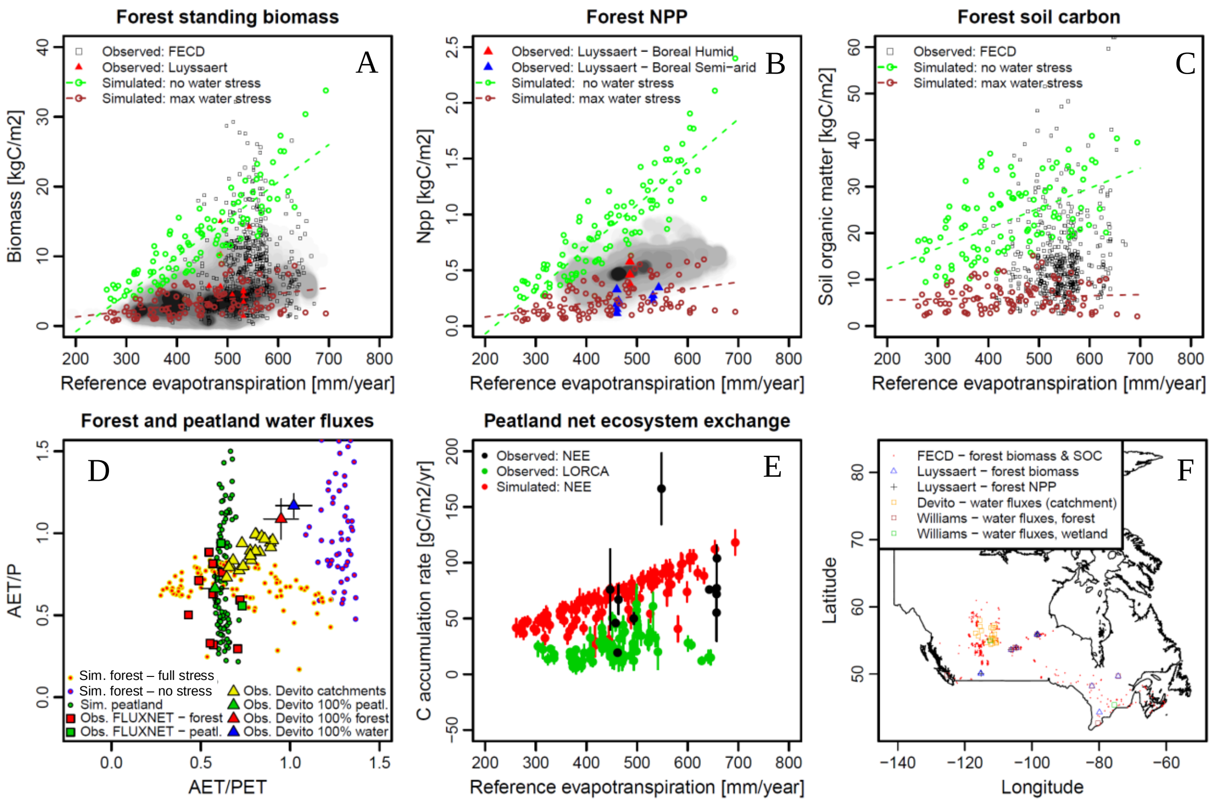

Figure S3.2 Model validation results for forest and wetland ecosystem properties with Canadian Datasets.

A) *Modelled forest biomass was compared with 3 datasets of measured forest biomass. 1) Gridded forest biomass map at 250m×250m resolution (grey point clouds Beaudoin, et al., 2014); 2) Forest ecosystem carbon database (FECD; Shaw et al., 2005). 3) Luyssaert dataset (Luyssaert et al., 2007). For all observations tree locations with a standage older than 60 years were selected. Simulated biomass is shown for forests with optimal water supply (no water stress) and forests that cannot reach groundwater (max water stress).*

B) Modelled forest net primary productivity (NPP) were compared with 1) Gridded forest NPP map at 0.01°×0.01° resolution (grey point clouds Thurner et al., 2017); and 2) Luyssaert dataset (Luyssaert et al., 2007).

C) Modelled forest soil carbon were compared with observations from the Forest ecosystem carbon database (FECD; Shaw et al., 2005).

D) Simulated forest and peatland water fluxes were compared to 2 types of measured water fluxes. Catchment level water fluxes derived from river discharges in the Boreal Plains (Devito et al., 2017), and the derived estimates for hypothetical catchments with 100% forest, peatland, or open water (the whiskers indicate the uncertainty). 2) Forest and peatland water use derived from fluxnet sites (Williams et al,, 2012). Simulated water fluxes are shown for forests with optimal water supply (no water stress), forests that cannot reach groundwater (max water stress), and peatlands.

E) Modeled peatland net ecosystem exchange (NEE) of carbon was compared with observed long term rates of carbon accumulation (LORCA) for the last 1000 years, based on dating methods (Gallego-Sala et al., 2018), and observed NEE from a Canadian dataset (Webster et al., 2018).

S3.2 Evapotranspiration

The reference evapotranspiration (*PEt*) is an important climate variable in the model. We applied a Priestly-Taylor-type equation and calibrated the parameters of this equations to long-term average *PEt*-values throughout Sweden published by Van der Velde et al. (2012) and daily Reported Makkink-reference evapotranspiration for a single site in the Netherlands.

$$PEt = -0.0202 + \frac{1}{1280 \cdot 10^6}\left(0.5 \cdot \left[T\max + T\min\right] + 16.20\right) \cdot \left(T\max - T\min\right)^{0.51} \cdot S_{in}(lat)$$

*PEt =0.81*Makkink PEt*

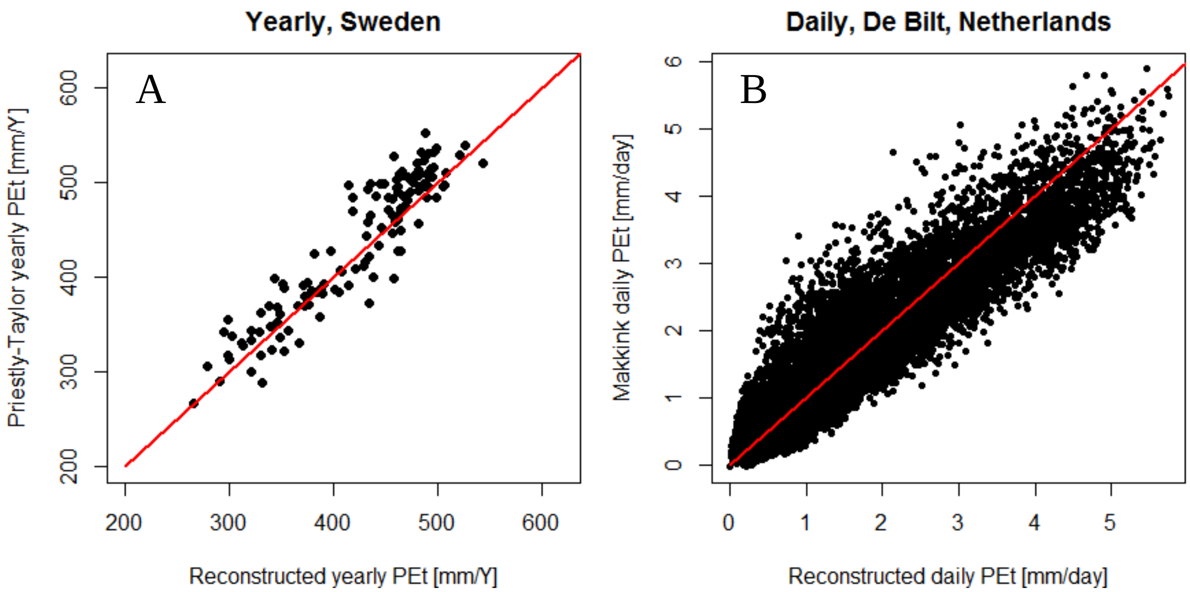

Figure S3.3 The parameters of Eqs S2.1 and S2.2 were calibrated to both long term average values for Sweden (Van der Velde et al., 2012)(A) as well as daily Makkink-Et values published by the KNMI for the Bilt (B). Both datasets were reproduced satisfactory

References

- Aurela, M., T. Laurila, and J. Tuovinen, 2004.The timing of snow melt controls the annual CO2 balance in a subarctic fen. GRL VOL. 31, L16119
- Beaudoin, A., Bernier, P. Y., Guindon, L., Villemaire, P., Guo, X. J., Stinson, G., Bergeron, T., Magnussen, S. and Hall, R. J.: Mapping attributes of Canada's forests at moderate resolution through k NN and MODIS imagery, Canadian Journal of Forest Research, 44(5), 521–532, doi:10.1139/cjfr-2013-0401, 2014.
- Billett, M.F., D. J. Charman, J. M. Clark, C. D. Evans, M. G. Evans, N. J. Ostle, F. Worrall, A. Burden, K. J. Dinsmore, T. Jones, N. P. McNamara, L. Parry, J. G. Rowson, R. Rose, 2010. Carbon balance of UK peatlands: current state of knowledge and future research challenges. Climate research Vol. 45: 13–29, 2010.
- De Wit, H.A. , J.L.J. Ledesma, M.N. Futter, 2016. Aquatic DOC export from subarctic Atlantic blanket bog in Norway is controlled by seasalt deposition, temperature and precipitation. Biogeochemistry (2016) 127:305–321
- Devito, K. J., Hokanson, K. J., Moore, P. A., Kettridge, N., Anderson, A. E., Chasmer, L., Hopkinson, C., Lukenbach, M. C., Mendoza, C. A., Morissette, J., Peters, D. L., Petrone, R. M., Silins, U., Smerdon, B. and Waddington, J. M.: Landscape controls on long-term runoff in subhumid heterogeneous Boreal Plains catchments, Hydrological Processes, 31(15), 2737–2751, doi:10.1002/hyp.11213, 2017.
- Drösler, M., 2005. Trace gas exchange and climatic relevance of bog ecosystems, Southern Germany, Dissertation TUM, 179 pp. Online publication: urn:nbn:de:bvb:91-diss20050901-1249431017.
- Gallego-Sala, A. V., Charman, D. J., Brewer, S., Page, S. E., Prentice, I. C., Friedlingstein, P., Moreton, S., Amesbury, M. J., Beilman, D. W., Björck, S., Blyakharchuk, T., Bochicchio, C., Booth, R. K., Bunbury, J., Camill, P., Carless, D., Chimner, R. A., Clifford, M., Cressey, E., Courtney-Mustaphi, C., De Vleeschouwer, F., de Jong, R., Fialkiewicz-Koziel, B., Finkelstein, S. A., Garneau, M., Githumbi, E., Hribjlan, J., Holmquist, J., Hughes, P. D. M., Jones, C., Jones, M. C., Karofeld, E., Klein, E. S., Kokfelt, U., Korhola, A., Lacourse, T., Le Roux, G., Lamentowicz, M., Large, D., Lavoie, M., Loisel, J., Mackay, H., MacDonald, G. M., Makila, M., Magnan, G., Marchant, R., Marcisz, K., Martínez Cortizas, A., Massa, C., Mathijssen, P., Mauquoy, D., Mighall, T., Mitchell, F. J. G., Moss, P., Nichols, J., Oksanen, P. O., Orme, L., Packalen, M. S., Robinson, S., Roland, T. P., Sanderson, N. K., Sannel, A. B. K., Silva-Sánchez, N., Steinberg, N., Swindles, G. T., Turner, T. E., Uglow, J., Väliranta, M., van Bellen, S., van der Linden, M., van Geel, B., Wang, G., Yu, Z., Zaragoza-Castells, J. and Zhao, Y.: Latitudinal limits to the predicted increase of the peatland carbon sink with warming, Nature Climate Change, 8(10), 907–913, doi:10.1038/s41558-018-0271-1, 2018.
- Helfter, C., C. Campbell, K. J. Dinsmore, J. Drewer, M. Coyle, M. Anderson, U. Skiba, E. Nemitz, M. F. Billett, and M. A. Sutton, 2015. Drivers of long-term variability in CO2 net ecosystem exchange in a temperate peatland. Biogeosciences, 12, 1799–1811
- Juutinen, S., M. Väliranta, V. Kuutti, A. M. Laine, T. Virtanen, H. Seppä, J. Weckström, and E-S. Tuittila 2013. Short-term and long-term carbon dynamics in a northern peatland-stream-lake continuum: A catchment approach, J. Geophys. Res. Biogeosci., 118, 171–183, doi:10.1002/jgrg.20028
- Luyssaert, S., et al, (2007), CO2 balance of boreal, temperate, and tropical forests derived from a global database. Global Change Biology, 13: 2509–2537. doi:10.1111/j.1365-2486.2007.01439.x
- Malmer, N. G. Svensson and B. Wallén, 2011. Carbon and mass balance in a south Swedish ombrotrophic bog: processes and variation during recent centuries. Mires and Peat, Volume 8, Article 01, 1–16,
- Olefeldt, D., N. T. Roulet, O. Bergeron, P. Crill, K. Bäckstrand, and T. R. Christensen (2012), Net carbon accumulation of a high-latitude permafrost palsa mire similar to permafrost-free peatlands, Geophys. Res. Lett., 39, L03501, doi:10.1029/2011GL050355
- Olsson, M.T., M. Erlandsson, L. Lundin, Torbjörn Nilsson, Åke Nilsson and Johan Stendahl 2009. Organic Carbon Stocks in Swedish Podzol Soils in Relation to Soil Hydrology and Other Site Characteristics. Silva Fennica 43(2)
- Shaw, C., Bhatti, J. S. and Sabourin, K. J.: An ecosystem carbon database for Canadian forests, Canadian Forest Service, Northern Forestry Centre., 2005.
- Thurner M, Beer C, Ciais P, et al.Evaluation of climate-related carbon turnover processes in global vegetation models for boreal and temperate forests. Glob Change Biol. 2017;23:3076–3091.https://doi.org/10.1111/gcb.13660THURNERET AL.|3091
- Turner, E.T., G.T. Swindles, K.H. Roucoux,2013. Late Holocene ecohydrological and carbon dynamics of a UK raised bog: impact of human activity and climate change. Quaternary Science Reviews 84, 65-85. doi: org/10.1016/j.quascirev.2013.10.030
- Turunen, J., E. Tomppo, K. Tolonen and A. Reinikainen, 2002.. Estimating carbon accumulation rates of undrained mires in Finland – application to boreal and subarctic regions. The Holocene 12,1 pp. 69–80
- Van der Linden, M., M.M.P.D. Heijmans and B. van Geel, 2014. Carbon accumulation in peat deposits from northern Sweden to northern Germany during the last millennium. The Holocene 1–9
- Van der Velde, Y., S. W. Lyon, and G. Destouni (2013), Data-driven regionalization of river discharges and emergent land cover–evapotranspiration relationships across Sweden, J. Geophys. Res. Atmos., 118, 2576–2587, doi:10.1002/jgrd.50224.

- Wang,M., J. Wu, P.M. Lafleur, J. Luan, H. Chen, X. Zhu, 2018. Can abandoned peatland pasture sequestrate more carbon dioxide from the atmosphere than an adjacent pristine bog in Newfoundland, Canada? Agricultural and Forest Meteorology Volume 248, 15 P 91-108
- Webster, K. L., Bhatti, J. S., Thompson, D. K., Nelson, S. A., Shaw, C. H., Bona, K. A., Hayne, S. L. and Kurz, W. A.: Spatially-integrated estimates of net ecosystem exchange and methane fluxes from Canadian peatlands, Carbon Balance and Management, 13(1), doi:10.1186/s13021-018-0105-5, 2018.
- Williams, C. A., et al. (2012), Climate and vegetation controls on the surface water balance: Synthesis of evapotranspiration measured across a global network of flux towers, Water Resour. Res., 48, W06523, doi:10.1029/2011WR011586
- Yu, Z., J. Loisel, D. P. Brosseau, D. W. Beilman, and S. J. Hunt (2010), Global peatland dynamics since the Last Glacial Maximum, Geophys. Res. Lett., 37, L13402, doi:10.1029/2010GL043584.
  .

Supplement 4 Sensitivity analysis

We performed an exploratory sensitivity analysis for all model parameters for 14 locations ranging from wet and cold (PET/P<1) to dry and warm (PET/P>1, figure S4.1). The sensitivity of the main model variables to the model parameters and drivers can be different for any climate. To explore this spatial pattern in sensitivity, we selected 14 locations with a strong gradient in PET/P and for each location we evaluated and increase and decrease of 5% of each of the 40 model parameters. Ctemp and Cprecip represent a 1 degree and a 5% change in temperature and precipitation respectively. We plotted the 6 parameters with the largest average (over the 14 locations) effects on the model results. For all four bi-stability variables (threshold exfiltration forest, threshold infiltration peatlands, restoration resistance and critical flux), the parameters describing the relation between biomass and ET, and between transpiration and water table for wetlands are most sensitive, followed by precipitation and temperature. Next to weather and transpiration parameters, we see a slight effect of Specific yield difference (note that in the figures below $Pp=Sy_p$) between mineral soil and peat soil for "minimum drainage forest".

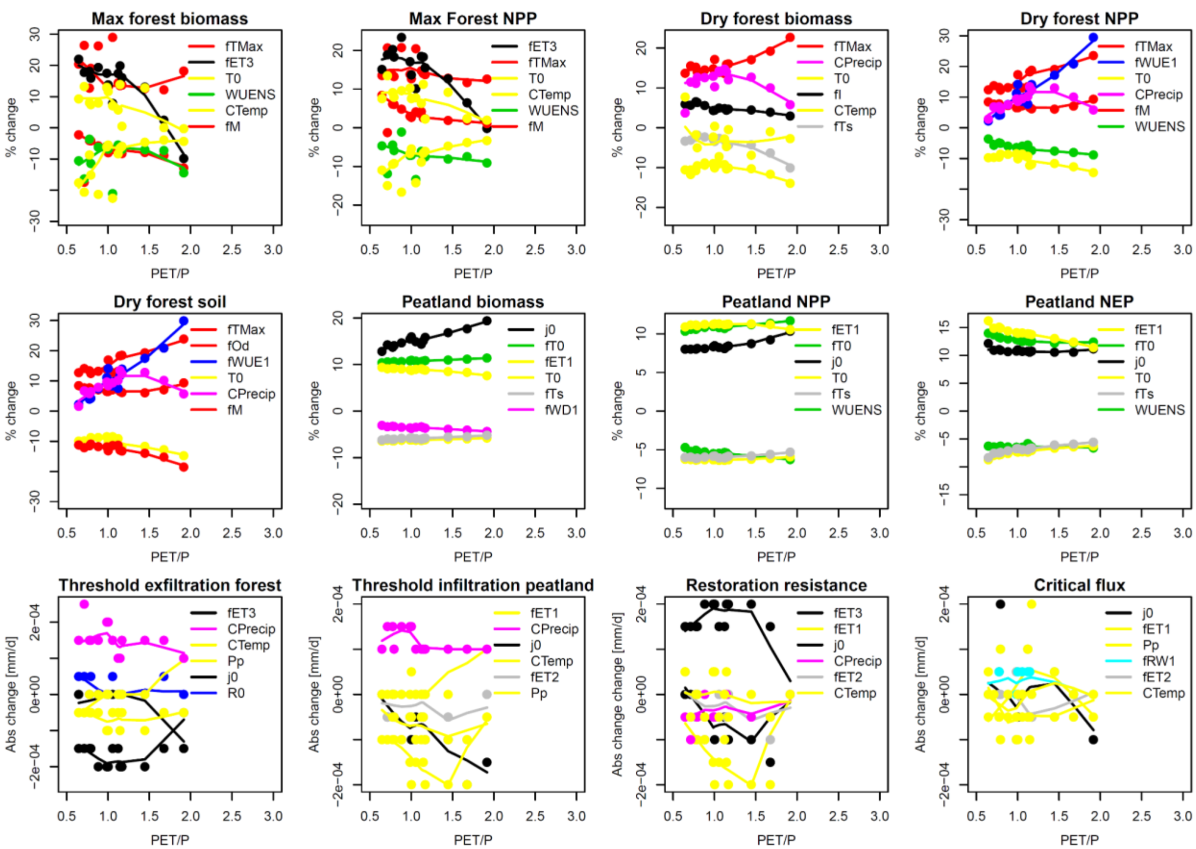

*Figure S4.1:. Explorative sensitivity analysis. Parameter names relate to table S1.3. CTemp stands for a +1 and -1 degree change in temperature, Cprecip for a +5% and -5% change in precipitation. All other parameters are varied from +5 to -5% of their estimated value. %change =([+5%] - [-5%])/[base]*100. The dots represent the actual calculated sensitivity values, while the lines are indicative for the spatial correlation* *between sensitivities. Any change of more than 10% indicates that a 10% change (-5%+5%) in parameter value results in a larger effect on the variable. The 6 most influential parameters are shown in the legend sorted from high to low impact.*

Additionally, a spatial correlation analysis of four model variables with climate was performed. For this analysis we correlated the climate (only driver for the spatial pattern)in a radius of 200km around each point to the model output 1) Threshold infiltration peatland, 2) Threshold exfiltration forests, 3) restoration resistance , and 4) Critical flux A correlation model was made for each location for each variable. We followed the order of the legend (Fig S4.2) with first the yearly average values and subsequently their standard deviation. When a subsequent variable had a 5% higher explained variance than the best explaining variable from the legend list upto that variable, this variable was assumed the strongest control. If no variable could explain more than 40% “no significant control” was assigned. . This figure shows that the restoration resistance range is controlled by the variability in yearly rainfall in western Europe, and by yearly average PET in Northern Europe. In eastern Europe the peat growth and its bi-stability range seems to be a complex balance between precipitation, temperature and Evapotranspiration. The critical flux is controlled both by the yearly average precipitation and PET for most of Europe.

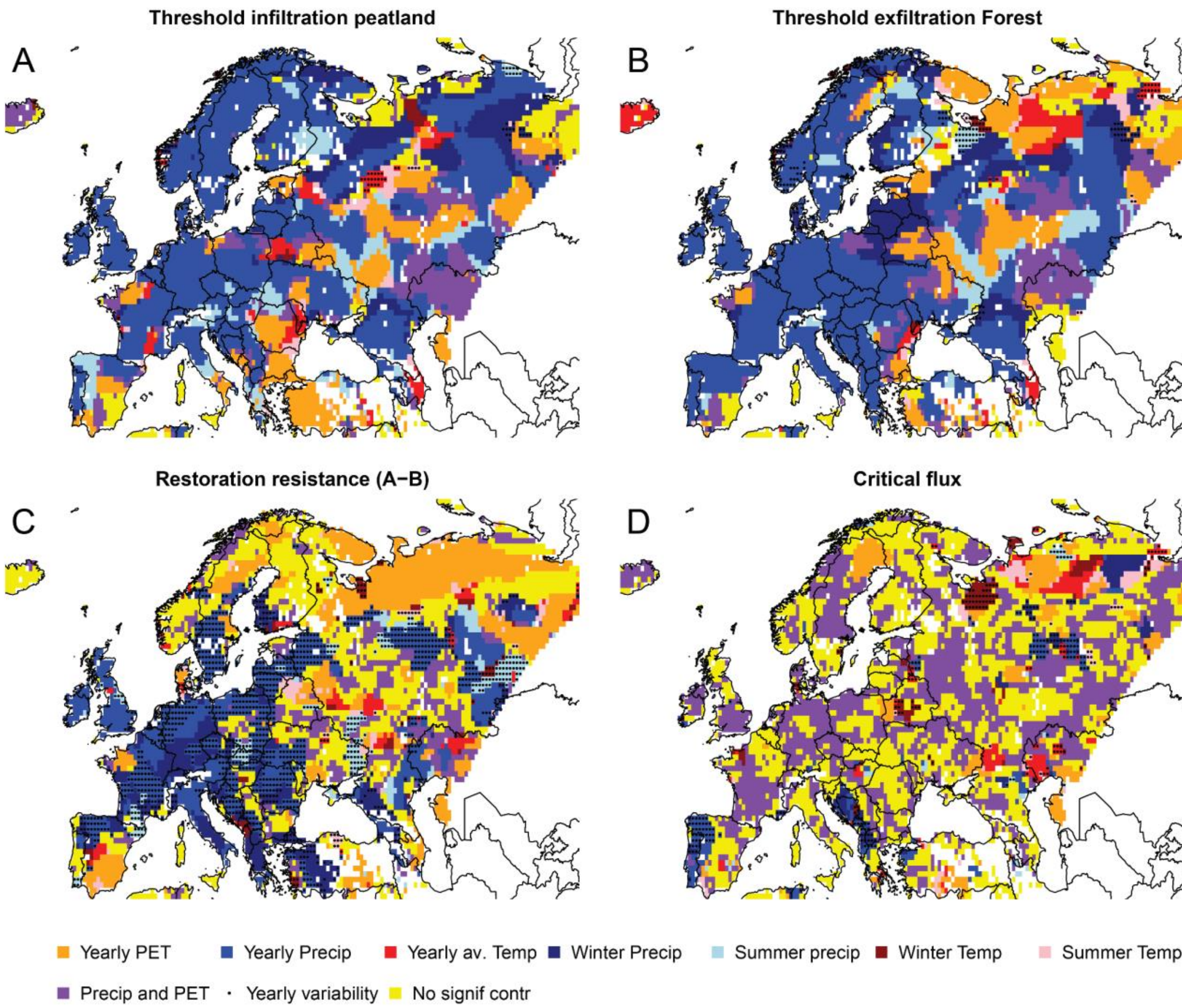

Figure S4.1: Spatial correlation analysis between climate and bi-stability variables.

Model sensitivity analyses (S4.1) reveals that the threshold infiltration for peatlands and the restauration resistance are more sensitive to parameters that describe transpiration and thus growth difference between peatlands and forests than to water storage differences between peatlands and mineral forest soils. Next to evaporation parameters, the critical flux is also sensitive to the runoff resistance and the evaporation flux during ponding which directly relate to ponding dynamics. A higher degree of ponding leads to a lower critical flux and therefore a more resilient peatland. An additional spatial correlation analysis shows that the dominant climate control on resistance is yearly variability in precipitation and winter precipitation in West and Central Europe, potential evapotranspiration in Northern Europe, and a complex set of controls in Eastern Europe (fig. S4.2). Spatial differences in the critical flux are controlled by both precipitation and potential evapotranspiration in most of Europe. This indicates that there are many aspects of climate change that may affect resilience of peatlands, with potentially contrasting effects over relatively short distances, especially in Eastern Europe.

Supplement 5. Estimate of potential carbon loss.

We propose back-of-the-envelope estimates of the amount of carbon that we expect to be released to the atmosphere when the raised bogs in the "highly sensitive" zone shift to a "valley fen" landscape. We base our estimate on the detailed soilgrids database (Hengl et al., 2014) that give a global soil Carbon stock estimate with a 1x1 km resolution. It is a conservative estimate because this dataset only contains estimated carbon stocks for the first 2 meters of soil, while raised bogs are known to grow up to 12m thick. However, we are not aware of datasets better representing the carbon stocks of peatlands. As this dataset covers the first 2m of soil, compared to the 1m that many other datasets include, total global carbon stocks for this dataset are relatively high (518Pg versus e.g. 2470 Pg of the Harmonized World Soil Database(Hiederer & Köchy, 2011)). This has to be taken into account interpreting our numbers, but the overall high soil carbon store is not expected to affect relative numbers much. 66% of all soil carbon in the Soilgrids dataset is found north of 35° latitude and 32% north of 60° latitude.
We combined these estimates with the number of peatlands found in each of the simulated peatland zones based on the Natura2000 dataset. This dataset does not allow to calculate accurate peatland areas for entire Europe, but it is a completely in depend dataset based on vegetation recording and as such extremely valuable. For comparing simulated peatland types with observed peatland types in Fig. 2 we only used peatlands with Representativity-class "A": the peatlands truly representative for its type. For raised bogs the number of "representative" raised bogs are shown in table S5.1

Table S5.1 Summary Table of simulated potential peatland areas, their average carbon content, total carbon content and observed peatland numbers from the Natura2000 dataset.

	Area (*10^6 km^2)	Mean C (kg/m^2)	Total C (Ptg)	Nr peatlands/$10^4 m^2$	Nr "A" RB /$10^4 km^2$
BB	0.20	74	14.7	21.1	-
BF	1.33	128	171	20.1	-
RB	3.75	62	235	17.9	3.1
RBr	1.15	56.6	65.5	20.9	4.0
RBs	1.48	71	107	15.7	2.3
RBhs	1.10	57	63	12.8	1.8
VF	5.25	35	186	7.7	-
Tundra	0.55	90	50.1	5.9	-
Total	11.05	59	655	13.5	-

BB= Blanket Bog, BF= Boreal Fen, RB= Raised Bog, RBr = robust Raised bog, RBs = Sensitive Raised Bog, RBhs= Highly sensitive Raised Bog, VF= Valley Fen

"highly sensitive" Raised bog zone
Average carbon stock: **57** Kg C/m^2
Total area: 1.100.000 km^2

“Valley fen” zone

Average carbon stock of the Valley fen zone with a dryness index (PET/P) smaller than 2. This is the zone just south of the “highly sensitive” zone: **35** kg C/m^2

Our rough estimate of the amount of carbon released: **57** - 35 = **22** kg C /m^2.

Potential amount of Carbon released due to shift between highly sensitive Raised bog and Valley fens:

(57 – 35) * 1000 * 1.100.000* 1*10^6 = 24.2 Pg C

Estimated number of peatlands affected through this conversion:

(12.8 – 7.7) * 110= 561

Estimated number of “A”-type Raised bogs affected through this conversion:

1.8 *110 = 198

Supplement References

Bartholomeus, R. P., Witte, J.-P. M., van Bodegom, P. M., van Dam, J. C., & Aerts, R. (2008). Critical soil conditions for oxygen stress to plant roots: Substituting the Feddes-function by a process-based model. *Journal of Hydrology*, *360*(1–4), 147–165. https://doi.org/10.1016/j.jhydrol.2008.07.029

Beckwith, C. W., Baird, A. J., & Heathwaite, A. L. (2003). Anisotropy and depth-related heterogeneity of hydraulic conductivity in a bog peat. I: laboratory measurements. *Hydrological Processes*, *17*(1), 89–101. https://doi.org/10.1002/hyp.1116

Bourgault, M.-A., Larocque, M., & Garneau, M. (2017). Quantification of peatland water storage capacity using the water table fluctuation method. *Hydrological Processes*, *31*(5), 1184–1195. https://doi.org/10.1002/hyp.11116

Clymo, R. S. (1984). The Limits to Peat Bog Growth. *Philosophical Transactions of the Royal Society B: Biological Sciences*, *303*(1117), 605–654. https://doi.org/10.1098/rstb.1984.0002

Collins, E. H. (1934). Relationship of degree-days above freezing to runoff. *Transactions, American Geophysical Union*, *15*(2), 624. https://doi.org/10.1029/TR015i002p00624-2

Feddes, R. A., Hoff, H., Bruen, M., Dawson, T., de Rosnay, P., Dirmeyer, P., et al. (2001). Modeling Root Water Uptake in Hydrological and Climate Models. *Bulletin of the American Meteorological Society*, *82*(12), 2797–2809. https://doi.org/10.1175/1520-0477(2001)082<2797:MRWUIH>2.3.CO;2

Frolking, S, Roulet, N. T., Tuittila, E., Bubier, J. L., Quillet, A., Talbot, J., & Richard, P. J. H. (2010). A new model of Holocene peatland net primary production, decomposition, water balance, and peat accumulation. *Earth System Dynamics*, *1*(1), 1–21. https://doi.org/10.5194/esd-1-1-2010

Frolking, Steve, Roulet, N. T., Moore, T. R., Richard, P. J. H., Lavoie, M., & Muller, S. D. (2001). Modeling Northern Peatland Decomposition and Peat Accumulation. *Ecosystems*, *4*(5), 479–498. https://doi.org/10.1007/s10021-001-0105-1

Hengl, T., de Jesus, J. M., MacMillan, R. A., Batjes, N. H., Heuvelink, G. B. M., Ribeiro, E., et al. (2014). SoilGrids1km — Global Soil Information Based on Automated Mapping. *PLoS ONE*, *9*(8), e105992. https://doi.org/10.1371/journal.pone.0105992

Hiederer, R., & Köchy, M. (2011). *Global soil organic carbon estimates and the harmonized world soil database*. *EUR 25225EN, Luxembourg*. https://doi.org/10.2788/13267

Kätterer, T., Andrén, O., & Jansson, P.-E. (2006). Pedotransfer functions for estimating plant available water and bulk density in Swedish agricultural soils. *Acta Agriculturae Scandinavica, Section B - Plant Soil Science*, *56*(4), 263–276. https://doi.org/10.1080/09064710500310170

Kleinen, T., Brovkin, V., & Schuldt, R. J. (2012). A dynamic model of wetland extent and peat accumulation: results for the Holocene. *Biogeosciences*, *9*(1), 235–248. https://doi.org/10.5194/bg-9-235-2012

Lafleur, P. M., Hember, R. A., Admiral, S. W., & Roulet, N. T. (2005). Annual and seasonal variability in evapotranspiration and water table at a shrub-covered bog in southern Ontario, Canada. *Hydrological Processes*, *19*(18), 3533–3550. https://doi.org/10.1002/hyp.5842

Moors, E. J. (2012). Water Use of Forests in the Netherlands, 290.

Mueller, L., Behrendt, A., Schalitz, G., & Schindler, U. (2005). Above ground biomass and water use efficiency of crops at shallow water tables in a temperate climate. *Agricultural Water Management*, *75*(2), 117–136. https://doi.org/10.1016/J.AGWAT.2004.12.006

Roebroek, C. T. J., Melsen, L. A., Van Dijke, A. J. H., Fan, Y., & Teuling, A. J. (2020). Global distribution of hydrologic controls on forest growth. *Hydrology and Earth System Sciences*, *24*(9), 4625–4639. https://doi.org/10.5194/hess-24-4625-2020

Siteur, K., Eppinga, M. B., Karssenberg, D., Baudena, M., Bierkens, M. F. P., & Rietkerk, M. (2014). How will increases in rainfall intensity affect semiarid ecosystems? *Water Resources Research*, *50*(7), 5980–6001. https://doi.org/10.1002/2013WR014955

Tang, X., Li, H., Desai, A. R., Nagy, Z., Luo, J., Kolb, T. E., et al. (2015). How is water-use efficiency of terrestrial ecosystems distributed and changing on Earth? *Scientific Reports*, *4*(1), 7483. https://doi.org/10.1038/srep07483

Teuling, A. J. (2017). A forest evapotranspiration paradox investigated using lysimeter data, 1–24. https://doi.org/10.2136/vzj2017.01.0031

van der Velde, Y., de Rooij, G. H., Rozemeijer, J. C., van Geer, F. C., & Broers, H. P. (2010). Nitrate response of a lowland catchment: On the relation between stream concentration and travel time distribution dynamics. *Water Resources Research*, *46*(11). https://doi.org/10.1029/2010WR009105

Van Der Velde, Y., De Rooij, G. H., & Torfs, P. J. J. F. (2009). Catchment-scale non-linear groundwater-surface water interactions in densely drained lowland catchments. *Hydrol. Earth Syst. Sci*, *13*, 1867–1885. Retrieved from www.hydrol-earth-syst-sci.net/13/1867/2009/

Vrugt, J. A., Dekker, S. C., & Bouten, W. (2003). Identification of rainfall interception model parameters from measurements of throughfall and forest canopy storage. *Water Resources Research*, *39*(9). https://doi.org/10.1029/2003WR002013